AN INTRODUCTION INTO THE MECHANICAL BEHAVIOR OF PAINTINGS UNDER RAPID LOADING CONDITIONS

Marion F. Mecklenburg and Charles S. Tumosa

ABSTRACT: *Paintings exposed to vibration or impact due to handling and transportation are often considered to be at risk for damage. This study examines some of the mechanical properties of typical artist materials under different environmental conditions and using that information, conducts a computer based analysis of representative paintings subjected to impact and vibration. The findings of the study indicate that paintings have a substantial intrinsic dynamic strength and that within reasonable limits the objects are generally able to withstand considerable sustained vibration as well as rather serious impact. Some conditions that merit special attention are examined.*

INTRODUCTION

If a painting is subjected to vibration, or dropped such that it will suffer a sudden impact, there will likely be a displacement of the painting out of the plane defined by the stretcher. In addition, paintings dropped on their edge can experience an in-plane distortion of the paint, ground, glue, and fabric composite layer. The severity of the distortion encountered during vibration results from the orientation of the painting to the vibration source and the closeness of match to the source vibration frequency of one of the natural or resonant frequencies of the painting. Any displacement or distortion of the painting, whether accidental or intentional, such as hammering out corner keys, necessarily distorts the materials that make up the painting, and as a consequence, induces stresses. If the stresses are high enough the materials fail, usually in the form of cracked and flaked paint. Relating the severity of the dynamic environment to the painting displacements, material distortions and ultimately the magnitude of the stresses developed in the layers of a painting is a study in engineering mechanics. In order to accomplish this, it is necessary to either measure or calculate the stresses in a vibrating painting and compare those stresses to the maximum the materials can sustain.

Clearly, it is not feasible to test paintings in the various collections around the world to determine the severity of shock and vibration that will cause design layer cracking. Other methods are necessary. A systematic engineering approach to solving the problem is available and requires specific steps. First, an analytical procedure must be found that determines the deformations and stresses in any of the layers of a painting subjected to vibration and impact. In this case computer modeling in the form of *Finite Element Analyses* (FEA) will be used. Second, the general dynamic mechanical properties of the artists' materials must be determined under different temperatures and relative humidities expected to be encountered under normal transport conditions. Third, a correlation between vibration and impact stimulus must be developed and the failure levels of the painting materials such that a *risk assessment* may be conducted that allows for the safe packing and transport of the work of art. While there is considerable literature on the mechanical

properties of commercial paints used as protective coatings,[1] there is not an abundance of information regarding the strength or stiffness of artists' materials under dynamic conditions. Some of this information has been determined at the Conservation Analytical Laboratory (CAL) by direct materials testing and yet more still needs to be done. The following is a summary of some of the information currently available.

MECHANICAL PROPERTIES OF MATERIALS

There are often misconceptions regarding the properties of solid materials. The mechanical properties of materials are frequently confused with their physical properties. The physical properties of materials refer to those such as density, color, luster, and atomic or molecular structure. Moisture-related swelling properties and the thermal coefficient of expansion also fall under this heading. The mechanical properties of a material refer to the strength, stiffness or flexibility, and elastic or plastic properties of materials.

The mechanical properties of materials can be quite specifically defined, and in fact, these properties can be quantified. For example, the stiffness of a material directly relates the amount of deformation, δ , (the stretched length, L_s, minus the unstretched length, L_o), a material undergoes when subjected to a force, F. If the applied force is large enough, then the material will break, and thus the strength of the material is determined. The difficulty with using the terms force and deformation arises when comparing one material to another. All of the specimens must be the exact same size and this is not always possible to accomplish. For example, comparing the mechanical properties of a thin paint film to a sample of hide glue means casting the materials so they both dry to the same dimensions which is nearly impossible. To get around this problem, the mechanical properties are "normalized." This is done by dividing the specimen deformation, δ, by the unstretched length of the specimen, L_o. This is the definition of engineering strain, ε, or mathematically:

$$\varepsilon = \frac{L_s - L_o}{L_o} = \frac{\delta}{L_o}$$

If the applied force, F, is divided by the cross-sectional area, A, of the test specimen, the term stress, σ, is thus defined:

$$\sigma = \frac{F}{A}$$

The ratio of stress to strain is the measure of the stiffness of the material, and for elastic material behavior, the modulus of elasticity, E, is how material stiffness is defined. Elastic behavior, simply stated, means a previously loaded material will return to its original length when the force is removed. Mathematically the modulus is:

$$E = \frac{\sigma}{\varepsilon}$$

A material is said to exhibit plastic properties when a permanent deformation occurs after the force is removed. The mechanical properties of a solid material are typically described using stress-strain diagrams, which are the result of direct specimen testing. One such plot is illustrated in Figure 1 (See *Appendix A* for all Figures). This figure shows the results of a tensile stress-strain test of a typical steel, which is one of the few materials that serve to demonstrate several points of interest on the same stress-strain test. This diagram shows the modulus of elasticity, E, as the slope of the linear (elastic) part of the plot, the yield point, δ, where plastic behavior begins, and the ultimate strength, δ_{ult} , the maximum stress the material can withstand.

Nearly all polymers such as paints and hide glue do not have clearly defined yield points, nor do they have such extended plastic regions.[2] More importantly, all of their mechanical properties are altered by temperature, relative humidity (RH), and the speed with which the force is applied to the specimen. Polymers often exhibit a "stress relaxation" once loaded and the strain fixed, this is in contrast to continued straining, or "creep," if loaded and the load is fixed. This time-dependent behavior of polymers is often referred to as visco-elastic effects.[3] At low temperatures and/or low relative humidity, these materials can behave in an ex-

tremely brittle, or "glassy," manner and conversely, at high temperature and relative humidity, they can be quite ductile or rubbery. At very high rates of loading they can also exhibit glassy and elastic behavior, demonstrating no yield point prior to failure. On the other hand when loaded slowly, the materials exhibit rubbery characteristics, with moderately large deformations.

MATERIALS TESTING

At CAL, a materials testing program has been underway for the last several years. This program was established to develop a data base of the mechanical properties of artists' materials. The information needed included long-term effects of temperature and relative humidity as well as the effects of loading rates and how they are affected by the same environmental factors. Additionally, some important information on the physical properties was determined. These included the dimensional response of the materials to temperature and relative humidity and the time required to achieve equilibrium to new environments. The materials tested to date include various pigmented artists' oil paints cast in 1978 and 1979, rabbit skin glues of different concentrations, various gesso mixtures, and linen textiles. Some wood testing was done, but as there is considerable literature on the mechanical properties of wood,[4] this discussion will only briefly include this aspect.

Sample Preparation

The oil paints were provided by the major manufacturers of artists' paints and were cast directly from the tube containers without the addition of any dryers, varnishes, or solvents. After thorough mixing, the paint was spread in 2.54 cm (1 in.) wide strips on .0127 cm (.005 in.) polyester film using strips of black vinyl electricians' tape as thickness guides. The tape was .0127 cm (.005 in.) thick and the paints were cast using both two and three layers resulting in paints of approximately .025 cm (.01 in.) and .038 cm (.015 in.) thicknesses. The thickness of the specimen affected the tensile test results while the paint was still less than four years old. There were no effects on the mechanical properties of the paints resulting from the two different thicknesses of paint for specimens over thirteen years old. This was a strong indication that the paints had dried uniformly throughout the thickness of the paints. The oils were typically linseed and safflower. Alkyds and acrylics were cast at the same time; however, testing on these materials is at present incomplete. The vinyl tape was removed after one month of drying time and the polyester was easily peeled away from the paint at the time of testing. The dry paint was then cut into strips .508 cm (.2 in.) wide and about 15.24 cm (6 in.) long for testing.

The rabbit skin glue samples were prepared by pouring 10% and 20% solutions (by weight) on the same type of polyester sheets as described above. These sheets were stretched tight onto flat, level surfaces. Once dry, usually after ninety-six hours at 23°C (73°F) and 50% RH, the glue specimens were cut to the similar dimensions as the paint. However, it was possible to obtain different thickness samples by simply cutting them from different areas of the casting. The different glue samples varied from .00381 cm (.0015 in.) to .0305 cm (.012 in.) in thickness. Gesso mixtures having different chalk-(ground calcium carbonate)-to-glue ratios were prepared from a single stock, 10% solution of rabbit skin glue. The gesso mixtures were cast and test samples were prepared in a manner similar to the glue.

Testing Equipment

The equipment used for conducting the tensile stress-strain tests of the materials was designed and constructed at CAL and can be generally described as miniature *screw-driven tensile machines.* The machines were small since the specimens to be tested were relatively small. The general layout of the equipment is illustrated in Mecklenburg (1984).[5]

As many as twenty-one of these devices were operating at any given time. It was necessary to have this many units because they often needed to be dedicated to a single

specimen for long periods of time. It took up to several months to generate some of the data if the specimens were to reach equilibrium with the test environment. All tests were conducted in chambers that provided controlled temperature and relative humidity. Conditioned silica gel was the primary technique for maintaining buffered environments.

Oil Paint Test Results

When it came to the actual testing, at least three specimens were initially tested to determine if the results would be consistent. Later testing showed that two specimens were sufficient, since the scatter was remarkably small, considering that the test materials were cast by hand. When variation did exist in the test results, it was usually the strain at failure. Specimens were tested at 3, 3.75, and 13 years after casting.

The tests undertaken were directed at specific questions: How are the mechanical properties of artists' materials influenced by temperature and relative humidity under very long term conditions? How are those mechanical properties affected by rapid loading events or dynamic conditions? and How does temperature and relative humidity influence the mechanical properties of materials subjected to dynamic conditions? The environments chosen emphasized low temperature and low relative humidity, because these conditions are where brittle behavior is most likely to be encountered.

While this paper will concentrate on dynamic systems, it is worth using the information on long-term material behavior as a baseline. This is best accomplished by examining the long-term or the "equilibrium" stress-strain test as illustrated in Figure 2.

In this test the paint specimen is rapidly strained a small amount, approximately .0007 (the units of strain are length per length or unitless), and the strain is fixed. The initial stress is recorded and the specimen then proceeds to stress "relax." This stress relaxation is a time-dependent phenomenon and takes about seven to ten days for the stress relaxation to cease or "equilibrium" is reached. The specimen is strained a subsequent increment and again allowed to fully stress relax. This process is continued until the specimen breaks, which in this case, took several months while the environment was maintained at 23°C and around 50% RH. Figure 3 shows the results of three specimens tested to failure. They are extremely consistent in terms of the modulus, but show a broad range of the failure strains which were .02, .026, and at least .034. This was the largest amount of scatter demonstrated by the test materials, and all of these strains are much larger than the calculated strains resulting from vibrations of a painting.

The locus of "relaxed" points (Figure 4) generated by the tests described above results in a stress-strain plot that is in equilibrium with the test environment and represents the mechanical properties of the material under extremely long-term conditions. The paint samples for all of the tests were prepared from a Naples yellow paint, which was, in fact, a lead carbonate tinted with cadmium sulfide and iron oxide ground in linseed oil. This paint was cast in March 1978.

Figure 4 clearly indicates there is no sharply defined yield point, but it appears to occur at approximately .414 Mega-Pascals (MPa) (60 pounds per square inch [psi]). The ultimate strength attained by this paint was 1.52 MPa (220 psi). The equilibrium modulus of this paint was about 68.94 MPa (10 ksi, 1 ksi=1,000 psi). This paint sample was able to "stretch" over 3.6% (strain x 100=percent elongation) of its original length. More on the equilibrium behavior of materials is discussed in the paper "The Mechanical Behavior of Paintings Subjected to Changes in Temperature and Relative Humidity."[6]

Also in Figure 4 are the results of rapidly run stress-strain tests of the same paint in the same environment. One of the tests was conducted with a separate test specimen, not previously tested and the other rapid test was conducted after the paint sample had been subjected to the very long-term tensile test. The most obvious observation is that in both rapid tests, the paint exhibits considerably more strength and is considerably stiffer

than in the equilibrium test. In this case, the paint attained strengths between 6.894 MPa and 7.58 MPa (1,000 psi and 1,100 psi). The previously untested paint had an elastic modulus of 689 MPa (100 ksi) and the previously tested paint was even stiffer with a modulus of 1,172 MPa (170 ksi). Apparently the long-term testing has "strain hardened" the paint. This behavior was exhibited on all of the paints tested except burnt sienna, which became less stiff. What is important is that these materials, even though subjected to long-term environmental testing, still have a dynamic reserve strength. They still develop considerable strength under rapid loading no matter what previous testing conditions were encountered.

Rapid Testing

After looking at the differences in behavior between the equilibrium and rapid mechanical properties, it is clear that the rate of loading has a pronounced influence. There does seem to be an upper limit on this influence. Loading the specimens faster than about .0005 cm/cm/sec at 50% RH and 23°C did not seem to appreciably affect either the modulus or the strength of the paint. The maximum modulus attained for the previously untested Naples yellow was 689 MPa (100 ksi) at several strain rates as shown in Figure 5. The testing procedure was to approximately double the strain rate for each subsequent test.

Additional results of the rapid loading tests conducted at 50% RH and 23°C are presented in Table 1 (See *Appendix B* for Tables). The first three paints listed in this table can be considered "fast driers" and the fourth and fifth, burnt sienna and burnt umber are "slow driers." Of the more than fifty paints (oils, whether linseed or safflower) cast in 1978 and 1979, only about 15% of the paints dried similar to the "fast dryers" and most of these contained lead. The "vermilion" tested was actually filled with a synthetically dyed calcium carbonate and presumably contained some dryer.[7] While not yet completely tested, titanium dioxide actually dried and remained quite flexible compared to the lead white. The balance of the paints are "slow dryers" and are still flexible at this time.

These testing results serve to demonstrate the considerable differences in mechanical behavior between the slow and fast driers. Another interesting aspect was the difference between the safflower and linseed oils. The linseed oils were able, at least in these tests, to elongate considerably more than the safflower oils. The safflower oil was found primarily in the white paints, presumably because it tends to discolor (yellow) less than the linseed upon drying. As the Naples yellow primarily contains lead carbonate, this paint offered a good comparison with the flake white ground in safflower. Finally, it is worth commenting that while a large proportion of paints used by artists are slow driers, and are quite flexible, a considerable number of paintings grounded with oil paints use white lead paint. This means that in many cases there is a fairly stiff paint layer between the glue size and the upper paint layers. If this paint substrate fails, then any layer above it will most likely fail also.

It is of some interest to know how these paints dry over time. In Table 2, test results are presented for the same paints as shown in Table 1, with the exception that the paints are considerably younger. The modulus of the younger paints are significantly lower than the thirteen-year-test paint in all cases.

The Effects of Temperature and Relative Humidity

Both cooling and desiccation increase the stiffness and strength of the materials tested. Tables 3a and b tabulate the influence of different relative humidity levels on the mechanical properties of two of the thirteen-year-old paints tested at 23°C. In both paints, desiccation at 5% RH shows the stiffest and strongest properties. Equally important is the reduction of the strain to failure. Clearly, the paints are losing their ability to deform without breaking. Under both environmental and dynamic conditions, the artists' material's ability to deform without

failure is our primary concern.

Cooling has an equally dramatic effect on the mechanical properties of these paints, (Tables 4a and b). At approximately -3°C, the materials are extremely brittle and relative humidity still affects these materials. Maintaining a relative humidity higher than the 51% reported was not possible with the equipment in use at the time of testing. The fast dryer, Naples yellow, showed relatively less response to relative humidity when compared to the slow dryer, burnt umber. Normally when testing a material, failure of the test specimen occurs as a single break. However, when testing at 5% RH and -3°C, the paints and hide glues shattered into multiple pieces. The hide glue disintegrated into over thirty separate pieces. These materials are acting in a truly "glassy" manner at this environment. On the other hand, the strengths of the materials measured at the cold environments were remarkably high.

Rabbit Skin Glue Test Results

At room temperature, relative humidity dramatically affects the mechanical properties of rabbit skin glue (Table 5). The *rapid-loading strength* of this material is remarkable in that it exceeds even the strongest epoxies at relative humidity levels above 60%.[8] Raising the relative humidity above this level causes a rapid decrease in the stiffness of the materials and at about 85% RH there is effectively no strength or stiffness in this material. The maximum strength and modulus attained was at 23°C and 5% RH, decreasing the temperature to -3°C at the same relative humidity effectively had little influence on the modulus but lowered the strength and strain to failure considerably. Hide glue specimens shattered in this environment and this was the first real evidence of a serious reduction of fracture resistance of these materials. Clearly this is an environment to avoid.

Gesso Test Results

Gesso is another material typically used as a ground on both panel and some fabric supported paintings.[9] The mechanical properties of this mixture of rabbit skin glue and whiting, in this case ground calcium carbonate, is affected by the ratio of pigment to glue. Some of the results of gesso testing are shown in Table 6. In this table the gesso mixture is expressed as the chalk-to-glue ratio, by weight, and the percent *pigment volume concentration,* (PVC). These mixtures can be compared to the modulus and strength of the glue alone (Table 5), where it is seen that the addition of the whiting increases the modulus, but decreases the strength considerably. At chalk-to-glue ratios greater than fifteen, both the strength and stiffness fall off severely. In comparison to the paints, the gesso is generally stiffer, but not quite as strong. In other words, it is more brittle. Since rabbit skin glue is the binder holding it together, gesso response to relative humidity will be also quite pronounced.

Support Materials

The mechanical properties of wood are well described in the literature since it is an important commercial material and used extensively as a structural material.[10] The one aspect of wood that is most important is that it is orthotropic, that is, it has considerably different mechanical properties in the mutually perpendicular directions, longitudinal, tangential, and radial. For example, oak, which along with poplar, was used as painting supports.[11] Oak can easily have a modulus of 6,894 MPa (1,000 ksi) in the longitudinal direction and approximately 551.5 MPa (80 ksi) in the other two directions. The strength of oak is equally different in the three different directions, about 96.5 MPa (14 ksi) in the longitudinal and only about 4.2 MPa (.6 ksi) in the other two. Hence, when it breaks it splits with the grain. The mechanical properties of wood vary, but in general they correlate somewhat with the density of the wood.[12] The most serious difficulties with wood is that it is so hygroscopic. Serious deviations in relative humidity can cause high stress levels in restrained panels, particularly when there is an existing crack.

In order to round out the materials, it is necessary to look at some of the properties of

textiles. Fabric painting supports are not homogeneous materials; they are a structure constructed of twisted bundles of fibers, yarns, woven together to form a mattlike structure. The difficulty presented by textiles arises when one is trying to numerically model them on a computer. Because of the type of woven structure, textiles tend to be considerably stiffer and stronger in the direction of the yarns, but are very flexible when subjected to bending. By using a volumetric analysis, it was possible to establish a mean fiber cross-section area per yarn. Using a large sample from the test fabric, the warp yarns were separated from the weft yarns and their separate volumes were measured using a nonpolar solvent. This volume was divided by the yarn length resulting in a total fiber bundle cross-section area. In turn, this total area was divided by the number of yarns resulting in a mean fiber cross-sectional area per yarn. By counting the yarns in a tensile test specimen, a mean fiber area could be obtained and enabling calculation of the mean fiber stress and modulus. This gave a better understanding of the fiber stresses than other types of measurements. Using three different linen textiles, #248 from Gernay-Delbec, #444 and #8800 from Ulster, the test results were remarkably close (Table 7).
It was found that the average yarn cross-sectional area was only about 22% of the nominal textile area if the area was taken to be the linen "thickness" times the specimen width. Typical linen thicknesses were .063 cm (.025 in.) for #248 and #444, and .048 cm (.019 in.) for #8800. For computer modeling purposes, the effective thickness of the fabric should only be about 22% of the measured nominal thickness. The effective modulus used in modeling should be those presented in Table 8.

The mechanical testing results of the #248 linen are shown in Table 8. This data is representative of all of the textiles tested. The strengths are not included because they are so high (considerably higher than the glue) that they are rarely a consideration except when the textile is extremely degraded. What is important is that the modulus of this material is considerably lower in the warp direction than the weft direction and the modulus tends to increase with relative humidity. This is the direct opposite of all of the other materials, which increase in stiffness with desiccation. Both of these properties are related to the fact that yarns are woven in the manufacture of a textile. The values of the warp yarns are so low because most of the early stretching is a result of straightening out the crimp. The weft direction, which has little crimp, is stiffer since the yarns are being stretched without additional straightening.

It must be noted that when a linen is stretched on a stretcher, the crimp is considerably reduced in the warp direction and slightly increased in the weft, so the mechanical properties tend to even out in the two orthogonal directions. Additionally, once stretched and subjected to high relative humidity, the initial fiber tension in the linen is considerably reduced due to interfiber slippage. This puts additional demands on the glue and the paints to support themselves.

COMPUTER MODELING

If a material is loaded, it will deform and the modulus describes the amount of deformation that will occur. If a structure is loaded, it also will deform and the amount of deformation is again a direct result of the modulus of the materials used in constructing the structure. Unfortunately, when many materials are involved or the geometry of the actual structure is complex, analysis of the structure is nearly impossible when using classical techniques of elastic theory. One method that provides remarkably good analytical results is the *Finite Element Analysis* (FEA) method.[13] This method mathematically approximates the structure on the digital computer by assembling the "structure" from smaller, geometrically simple "elements" whose mechanical properties can be determined. The elements are normally but not solely connected at the corners of the elements. These connections are called nodes. From elastic theory, force-displacement relationships can be established for individual elements. For example, it can be determined how much

stretching, bending, and twisting occurs when forces are applied to the nodes of the elements. If the element properties are formulated correctly, they can be assembled into a fairly complex structure using algebraic operations, which are easily handled by the computer. Further, convergence to the correct stresses and deflections will depend largely on the number of elements used in the model. For example, Figure 6 illustrates a simple cantilevered beam made of thick sheet acrylic plastic. The beam is supported at one end and a force of 1,334 Newtons (300 lbs.) is applied vertically at the other end. The dimensions of the beam are length, 45.7 cm (18 in.), height, 7.63 cm (3 in.), width, 2.42 cm (.95 in.). The modulus of this material used in the solutions was 3,102 MPa (450 ksi). From *beam theory*[14], which is one of the most thoroughly developed theories reflecting real-world accuracy, this beam will deflect 1.567 cm (.617 in.) downward at the free end and the maximum bending stresses will be plus or minus 26.2 MPa (3.79 ksi) at the fixed end. The maximum shear stresses will be 1.09 MPa (158 psi) occurring along the neutral axis (see Figure 6). The beam was modeled using FEA, but using different numbers of elements each time. The results of the analyses are shown in Tables 9a and b.

The final results of the solution using 360 elements agrees closely with theory and it is noteworthy that the solution for the deflection is converging to the correct answer from below, that is, the computed deflection will always be less than theoretical. On the other hand, the bending stresses will be higher, and this is the conservative solution. The measured failure stress of sheet acrylic is approximately 68.9 MPa (10 ksi) so it is possible to say that the force applied to this beam is only 39% of that needed to break it, according to this analysis. A risk analysis has now been conducted for the beam, which estimates that any force over 3,425 N (770 lbs.) will break the beam.

Sources of Forces under Dynamic Conditions

In the beam problem, it is easily seen that a weight hanging on the end of it can be the source of the applied force. For paintings subjected to vibration and impact, the forces are "inertial" and are not so readily envisioned. Isaac Newton, for whom the "Newton," the SI unit of force is named, determined that the force on a body is equal to its mass times the acceleration it experienced, or mathematically;

$$F = M \times a$$

On earth, the weight of an object is its mass times earth's gravitational field, g, or W=m x g. The mass of an object is defined as m=w/g. For a body experiencing vibration or shock, the forces it experiences are a result of its mass times the accelerations experienced. It is possible to say then, the force experienced, F_G, is:

$$F_G = \frac{W}{g} x\ a \text{ and}$$

$$F_G = W \times \frac{a}{g} \text{ and defining}$$

$$G = \frac{a}{g}$$

where G is the ratio of experienced acceleration to earth's gravity.

This G is the value to which is often referred when calculating inertial forces. For example to comment that an impact resulted in several G's, is to say that the impacted object is experiencing forces equivalent to G times the weight of the object. A dropped painting feeling 40 G's, then is said to act as if the painting is 40 times heavier than it actually is. For computer modeling purposes, a painting dropped on its edge experiencing 40 G's can have an applied force, totaling 40 times its weight, distributed over the entire area of the painting and in the direction parallel to the impact. It is necessary then to know how much the artist's materials weigh. See Table 10 for the nominal weight densities of some of the materials examined for mechanical properties.

The weight of any given painting per unit area will be the sum of the layer densities times the thickness of the respective layer. Expressed mathematically:

$$W_A = \Sigma\ (D_L\ x\ t_L)$$

Where:

W_A = the total weight of the painting per unit area.

D_L = the density of the layer.

t_L = the thickness of the layer

The dynamic loading on the painting per unit area will then be W_A times G. Its now possible to run an analysis of a model painting at room temperature, 23°C and 50% RH. The dimensions of the first painting are 76 x 102 cm (30 x 40 in.). The fabric is #248 with a nominal thickness of .0635 cm (.025 in.) therefore it weighs .0004 N/cm^2 (.0058 lbs./in.^{2}). The glue layer is .0076 cm (.002 in.) thick and weighs .0000508 N/cm^2 (.0000736 lbs./in.^{2}) and assume that the paint layer and ground is a total of .0178 cm (.003 in.) thick and is all white lead since it is the most brittle. The weight of the paint layer is .000213 N/cm^2 (.000309 lbs./in.^{2}). The total weight of the painting per unit area is .000664 N/cm^2 (.00618 lbs./in.^{2}) which is not very much, but this might be considered moderately thick for a paint film. At a 30 G impact, the painting will feel as if it weighs .012 N/cm^2 (.1855 lbs./in.^{2}).

All of the information needed for a FEA on the computer is now available. The model was assembled using 300 elements and 484 nodes and the three different layers are as described above with the exception that the model thickness of the linen is .01524 cm (.006 in.) and a mean modulus of 690 MPa (100 ksi) was used. All other material properties are described in the preceding tables for 23°C and 50% RH. The computer program is ANSYS, Version 4.4, leased by CAL and is run on a Gateway 2000 desktop PC. The computer uses 80386 technology at 33 MHz. It has a math coprocessor, an expanded RAM of 4 megabytes and a hard disk of 150 megabytes. The following modeling results are intended to examine the effects edge impact and out-of-plane vibration on the various layers of the painting.

Edge and Corner Impacts, the 76 x 102 cm Model Painting

A 76 x 102 cm (30 x 40 in.) painting was modeled first to examine the effects of a 30 G impact when dropped squarely on the long edge. ANSYS has a feature that allows programming in of the *mass* densities of the materials and then subjecting the model to any desired acceleration. Further, the painting was modeled such that the stretcher was firmly fixed and extremely rigid so that only the painting itself would respond to the impact without external influences such as stretcher distortion. In this way it is possible to look at the response of the painting alone. As with most real paintings, only the fabric was attached at the edges. This model and all subsequent model analysis performed assume that there are no pre-existing cracks in the paint film and all of the painting models have no auxiliary supports such as linings. The distorted painting is shown in Figure 7 along with the first layer element arrangement (the paint layer).

The maximum deflection is quite small, only .019 cm (.0075 in.). The maximum displacement of the paint layer is downward, only about .019 cm (.0075 in.) at the center of the painting. It actually deflected forward also, .0127 cm (.005 in.). The maximum stress the paint layer experienced is only .11 MPa (.016 ksi), which is less than 3% of the measured rapid loading breaking strength of the white lead paint, which is the lowest strength measured of the brittle paints. The distribution of the stresses is presented in Figure 8, and if the impact was ever large enough to actually break the paint, well over a 1,015 G impact, the theoretical crack pattern is shown in Figure 9 superimposed over the maximum principal stress vectors. In reality, this would most probably never occur, since buckling of

the painting out of the plane of the stretcher would be a more likely result of a high G impact. However unlikely that this crack pattern is, it is conceivable that very heavy traditional linings on very large paintings, could over a long period, cause this type of failure.

The same 30 G drop was modeled on the same painting except the orientation of the painting is with the diagonal vertical, Figure 10. Again the stretcher was rigid and fixed. The results were that the stresses again did not exceed .11 MPa (.016 ksi). The distribution of stresses from the 30 G corner impact and extremely high impact theoretical crack pattern are presented in Figures 11 and 12, respectively. These models suggest that factors other than the mass of the painting alone must intervene before impact can damage the paint layer.

Corner Impact of a 61 x 61 cm Painting with a Traditional Wood Stretcher and Fixed at the Corners

A smaller painting (61 x 61 cm [24 x 24 in.]), and therefore a lighter one, was modeled as if it were also subjected to a 30 G impact on its corner. In this case, a wood stretcher was included in the model with 2.54 x 7.62 cm (1 x 3 in.) stretcher bars. The corners of the stretcher were fixed as if they had been secured with screws, and in reality this describes a strainer. The post-impact distortion of the model painting is shown in Figure 13, and as can be seen, the painting reconfigured from a square to a diamond shape.

The maximum principal stresses in the paint film reached nearly 1.38 MPa (.2 ksi) or 37% of the measured breaking strength of the white lead paint. The complete stress distribution is shown in Figure 14 and the theoretical crack pattern is shown in Figure 15 if the impact exceeded 82 G's, which is quite possible.

The results of this test model has been compared to the test results provided by Paul Marcon, who made a model test drop of a painting at the Canadian Conservation Institute (CCI).[15] The computer model crack pattern is nearly identical to the experimental results. The indication here is that the stretcher, even if it is fixed at the corners, is sufficient to present a hazard to the painting if it is dropped on its corner. The wood stretcher bars are simply too flexible to prevent the type of distortion seen in Figure 13. Any weight attached to the painting, such as the frame, will only serve to aggravate the situation if a stiff backing board is not attached to the reverse of the stretcher.

Out-of-plane Vibration

For a painting to sustain a continuous out-of-plane vibration during transport, certain conditions must exist. The source of the vibration, i.e. trains, trucks, and airplanes, must provide a continuous vibration and it must be at a frequency near one of the natural or harmonic frequencies of the painting. Paul Marcon [16] has examined the types of vibrations most likely to occur in the various transportation modes, which makes it somewhat unlikely that sustained vibration will occur in a painting. He does point out those circumstances where it is possible that the right conditions exist to be of some concern. Therefore, it is worth examining what might happen if sustained vibration were to occur. The worst case is when the primary frequency is matched and the entire painting is deflected either to one side of the plane of the stretcher bars or the other. Additionally, some bending stresses are encountered, and the paint layer is under greater tension when the painting is deflected towards the side of the design layer. First, a 61 x 61 cm (24 x 24 in.) model with the same layers as described previously was used to examine the effect of initial uniform tension on the out-of-plane vibration of the painting.

Some preliminary remarks are necessary before showing the results of the computer modeling. When any object vibrates out of its original plane, a phenomena called *stress stiffening* occurs. This means the displacement is considerably reduced due to the conversion of bending stresses to purely axial stresses as the object no longer lays in the initial starting plane. For example, a stretched wire may experience bending stresses as it is initially dis-

placed from a straight line, but the further it is displaced, the more the stresses become uniform through the axial direction of the wire. In a painting, the initial displacement may have the paint film in tension, the glue layer with no stresses, and the fabric in compression. At full displacement all layers are in tension. This occurs because the ends of the wire, or in our case the edges of the painting, are restrained from moving. The computer program cannot handle stress stiffening directly, but must increment the applied load gradually mathematically correcting the orientation (rotation) of the elements. The problem, therefore, takes considerably longer to solve; in this case, between thirty-five and sixty minutes, depending on the number of iterations required. Ten iterations usually solved the problem correctly.

The next factor to consider is the actual inertial force applied to the model. Uniform accelerations were used in these models; in actual conditions the accelerations are maximum at the center of the paintings and reduce when approaching the edges. This means that the results shown are more severe than would occur to an actual painting. Finally, it has been thought that a vibrating painting is damped by its effort to move air adjacent to the painting out of the way. This may not be significant. If a painting is vibrating at 20 Hz (cycles per second) and has a displacement of 1.27 cm (.5 in.), the maximum velocity the painting experiences is only about 5.7 KPH (3.5 MPH). This velocity is not sufficient to cause serious pressure development at the surface of the painting unless the painting is enormous, in which case the frequency will be considerably lower, or it is tightly sealed by a very rigid backing board at the reverse. In the latter case, the painting must be vibrating in its primary mode. The 10 G acceleration level used in the following models was chosen on the assumption that the amplification factor of the paintings was around 20, which was measured by Paul Marcon at CCI, and the maximum peak acceleration from sustained vibration delivered by a transportation mode was .5 G. Additional useful information regarding sustained vibration in transportation vehicles can be found in the literature.[17]

Out-of-plane Accelerations on a 61 x 61 cm Model Painting

A 10 G acceleration was applied to the 61 x 61 cm (24 x 24 in.) model painting which had different uniform tensions applied. This model painting was "stretched" with different tensions and subjected to 10 G vibrations. The construction of the model painting is the same as described in the section on edge drops. The 10 G acceleration occurs at the same time that the painting is fully displaced from the plane of the stretcher. The typical out-of-plane displacement of the entire painting is illustrated in Figure 16, where the painted surface is upwards. The typical stress distribution shown in Figure 17 and a theoretical crack pattern is shown in Figure 18. The illustrations presented are for the least initial tension in Table 11.

It is noteworthy that the stresses are fairly uniform over the entire surface with a variation between a minimum stress of .43 MPa (.062 ksi) to a maximum of .58 MPa (.085 ksi). The maximum stresses occurred at the edges a bit away from the corners and the minimum at the center of the painting. This uniformity was found throughout each of the model painting layers. The maximum stress results for each of the pre-stress levels is shown in Table 11. The deflections included in this table are the center of the painting, moving from the plane of the stretcher to the maximum displacement of the painted surface outward.

The most important observation to be made here is the differences in the paint layer stresses before and after the application of a 10 G acceleration, which ranges from .24 MPa to .34 MPa (.040 ksi. to .049 ksi.). This is less than the initial pre-stresses placed in the paintings before a vibration at 10 G's. Even then, the total paint film stresses never exceed 25% of the measured breaking strength of the white lead paint. It appears easier to damage the painting by stretching it than by vibrating it. Recall also that these stresses are greater than would actually occur in a real painting. Another point is the relatively high

glue stresses due to the high modulus, and the low fabric stresses, due to the low modulus. This demonstrates the major influence the modulus has on the stress development in a material.

Out-of-plane Accelerations on a 67 x 102 cm Painting

A much larger painting was modeled to examine the effects of a larger surface area and different G levels. The 67 x 102 cm (30 x 40 in.) painting described in the section of the edge and corner impact was subjected to 1, 5, and 10 G accelerations at a fixed initial tension. The initial uniform pre-tension was induced by uniformly expanding the model painting .057 cm (.0225 in.) in the short direction and .07 cm (.03 in.) in the long direction. This resulted in initial pre-stresses in the layers of .517 MPa (.075 ksi) in the fabric, 3.09 MPa (.488 ksi) in the glue layer and .517 MPa (.075 ksi) in the paint layer. The calculated maximum stresses resulting from applying different G levels to this model are shown in Table 12. The net stress increases for the paint layer at the different accelerations are .28 MPa (.040 ksi), .29 MPa (.043 ksi), and .37 MPa (.053 ksi), which are not significant when considering the breaking strength of the paints. The application of a 1 G acceleration is the same as the painting would experience by simply resting face down on a table. The stresses in the paint film that developed under these circumstances is not much different than the 5 and 10 G accelerations and can be viewed as a result of the initial bending stresses that occur when the painting just begins to deflect from the in-plane position.

Even the deflections are not considerably different from the smaller painting modeled previously. The out-of-plane displacement computed is illustrated in Figure 19. The overall stress distribution resulting from the 10 G acceleration (Figure 20) is remarkably uniform as noted earlier in the smaller model and the theoretical crack pattern is shown in Figure 21.

Effects of Desiccation and Cooling

If the larger painting modeled above is subjected to desiccation and chilling while being subjected to a 10 G out-of-plane acceleration, the effects are considerable, and the results are primarily a consequence of the changes in the modulus of each material. The paint layer used in this model is the Naples yellow as the mechanical properties data is available and the properties of this paint is similar to the white lead previously used. The new stiffness values for the materials are now: the fabric 861 MPa (125 ksi), the glue 5,515 MPa (800 ksi), and the paint 4,019 MPa (583 ksi), which correspond to a 5% RH and -3°C environment. Also, because of the increase in the E values, the pre-stresses are significantly increased. The final analysis stress values are shown in Table 13. Of particular interest is the final stress of the paint film, which is 4.75 MPa (.690 ksi), which is considerably less than the strength of the Naples yellow and considerably less than the strength of this paint at this cold, dry climate (16.5 MPa [2.4 ksi]). Because of this large difference in the stresses, there is still a considerable safety factor from the vibration. It would be prudent to avoid this and any other environment that tends to stiffen the materials since there is a marked decrease in the strains to failure and inadvertent, though slight, blows directly to the painting surface will most likely cause damage.

Analysis of a 61 x 61 cm Painting with a Gesso Layer Replacing the Paint Film

If the paint film is replaced with gesso (PVC=93) at 23°C and 50% RH and subjected to a 10 G acceleration, the results reflect two major influences. The first is that the gesso only weighs about 36% of the white lead paint, so the forces resulting from the acceleration are less. The second and the most influential, is the modulus of the gesso is about 2.5 times greater than the paint and this appears to be the major consideration since the net stress increase (total minus initial) is .77 MPa (.112 ksi), which is over twice that experienced by the same size painting with a

paint layer. The results of this analysis are summarized in Table 14. The total calculated stress of the gesso (1.45 MPa [.211 ksi]) exceeds the breaking strength of the tested gesso (1.17 MPa [.170 ksi]) and suggest that this layer will start cracking. About half of this stress was a result of "stretching" the painting. The fact that we don't see crack patterns calculated by the computer analysis, suggests that the vibrations paintings encounter are not so severe.

SUMMARY

Artists' materials have rapid loading mechanical properties that vary with changes in temperature and relative humidity, becoming stiffer and stronger with drying and cooling. The paint is the weakest material in comparison to the glue and fabric, though depending on the mixture of chalk and glue, can be stronger than the gesso. The slow driers, burnt umber and burnt sienna, are so flexible that their ability to withstand deformation far exceeds the fast driers that contain lead carbonate or other driers. The primary concern are the lead-based paints, which are relatively stiff, having the higher modulus. The glue strengths are quite high and its failure will be extremely rare at ambient room temperature and at relative humidity level above 75%. This material has a strength of over twenty times the weaker lead paint at room temperature and 50% RH. If it does fail, it is almost a guarantee that the paint layer will also be destroyed.

At the coldest (-3°C) and driest (5% RH) environments, the materials tested shattered into multiple pieces even though the breaking strengths are quite high. At this environment, it is likely that the presence of pre-existing cracks in a painting composed of these materials might be a real concern, and further crack growth might be possible.

These initial results indicate that paintings constructed with even the stiffest and weakest thirteen-year-old lead paint can withstand fairly severe impacts if the stretcher is extremely rigid, otherwise the distortion of the stretcher will contribute to damaging the painting. Avoid any drop that allows a painting to hit corner first without any protection. The crack patterns predicted by the corner impact study where the stretcher is free to distort are easily reproducible on actual test paintings. Those crack patterns predicted by the stiffened stretcher model are not encountered in actual paintings.

The primary reason that the stress levels in paintings subjected to vibration are low, is the low total weight of the painted surface. This means a low mass, and inertial forces are in direct proportion to both the mass and the acceleration encountered. On the other hand, the added weight of the stretcher and frame, combined with the stretchers ability to deform are the reasons that damage is possible from a corner impact.

The modeling showed that the paintings were at very little risk from 10 G vibration should it occur. This was true even for the cold, dry environment, though this environment should be avoided at all costs. Even if paints become much stiffer and lose a considerable amount of their strength over the years due to slow evaporation of volatile components,[18] leeching of solubles from cleaning solvents, or other reasons, the stresses modeled by the computer are still insufficient to put the painting at serious risk. The stress due to vibration in any of the layers of the painting is remarkably uniform, but the analysis suggested that the highest stresses will occur at the edges and not in the middle. What theoretical crack patterns were developed by vibration modeling, have not been seen by the authors on any actual paintings. □

APPENDIX A — FIGURES

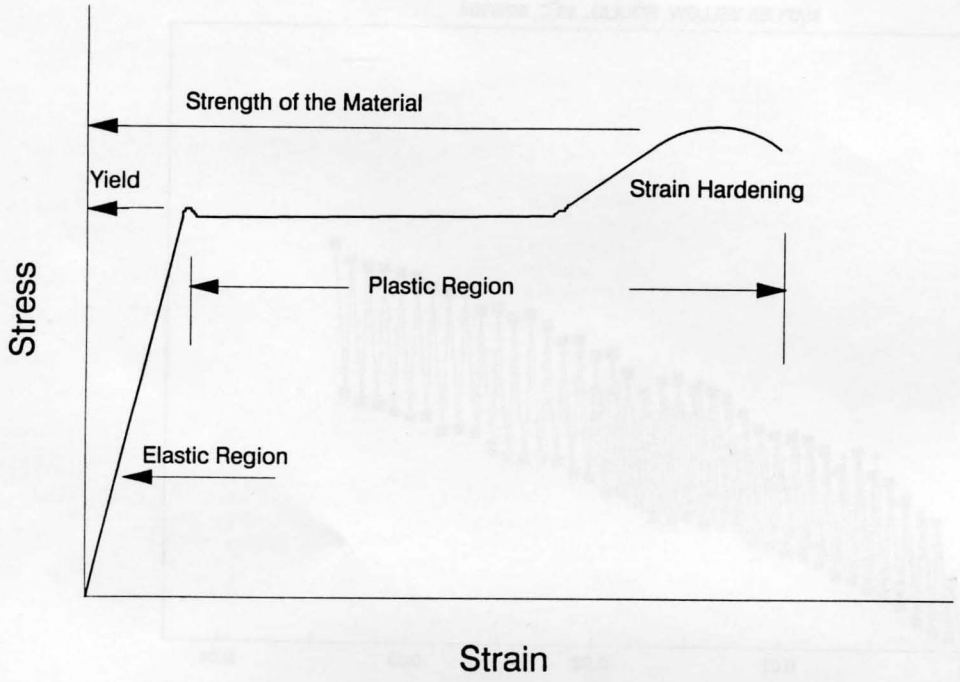

FIGURE 1
A typical stress-strain curve for a mild steel showing the major features of the mechanical properties of the material. Typical modulus for steel is 199,926 MPa (29,000 ksi) and the yield strength is 248 MPa (36 ksi). These are considerably higher than the polymers tested.

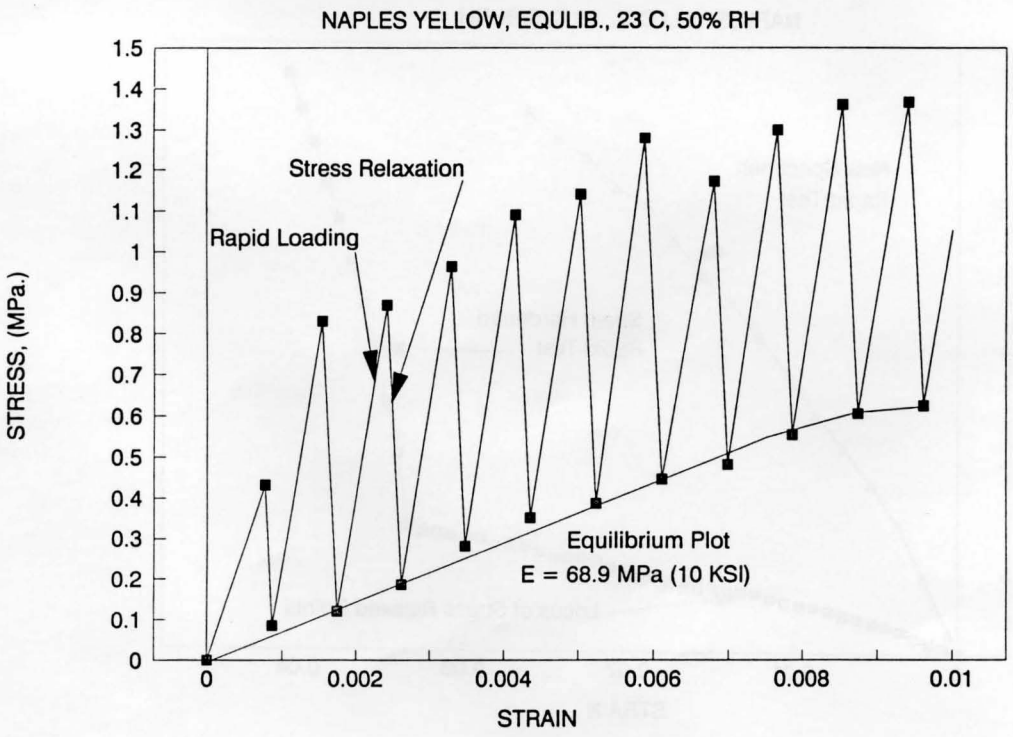

FIGURE 2
The typical test plot for establishing the "equilibrium" stress-strain data for artists' materials. Stress relaxation occurs after a rapid loading increment and the fully stress relaxed points establish the equilibrium stress-strain plot.

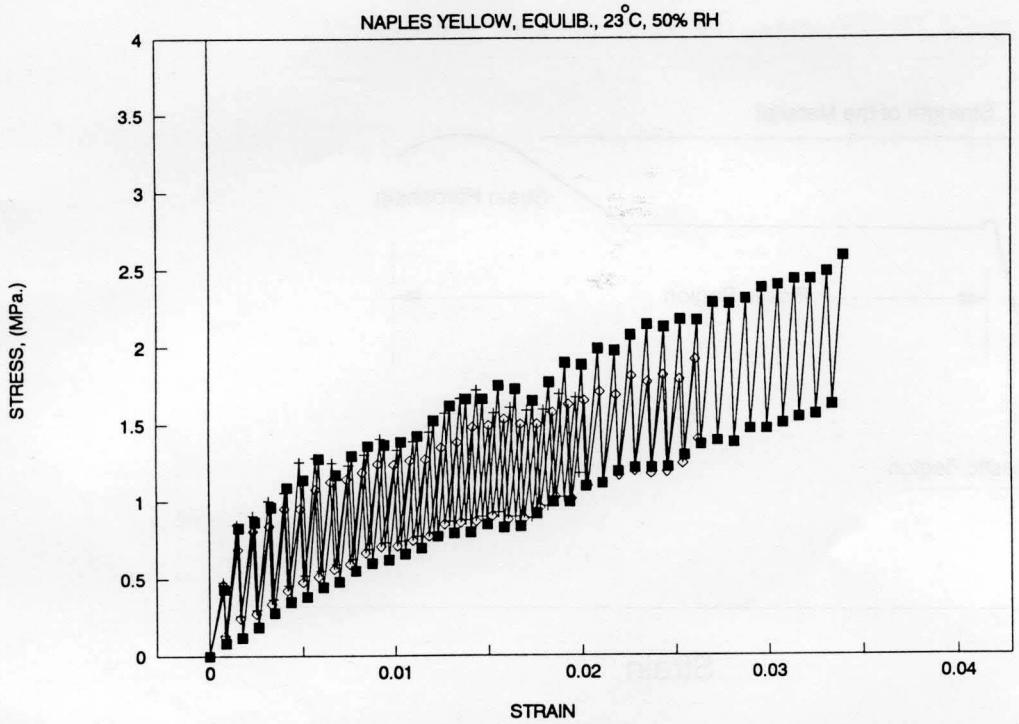

FIGURE 3
Equilibrium stress-strain tests results for three different samples of Naples yellow oil paint. This data represents the largest scatter observed in the materials testing. The slopes of the plots are quite consistent while the strain to failure is spread widely.

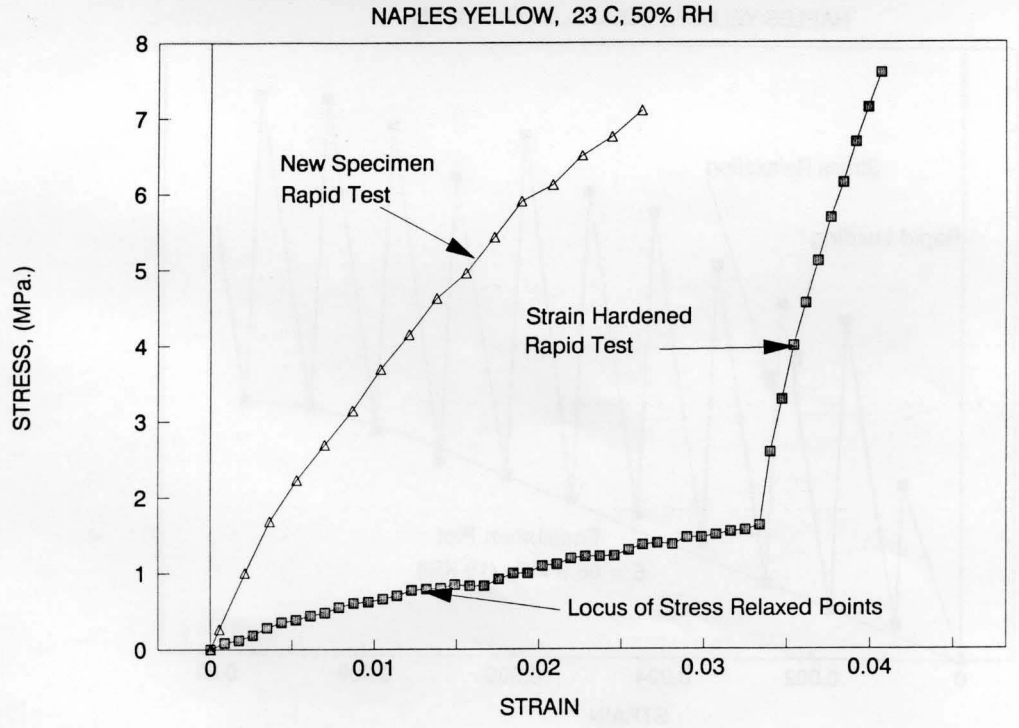

FIGURE 4
A comparison of the equilibrium stress-strain data to the rapid loading data. Rapid loading tests were conducted using both new specimens and specimens previously tested under equilibrium conditions. The differences in the stiffness and strength of the paint under these different loading conditions is considerable. There is still substantial rapid loading strength even after long-term testing.

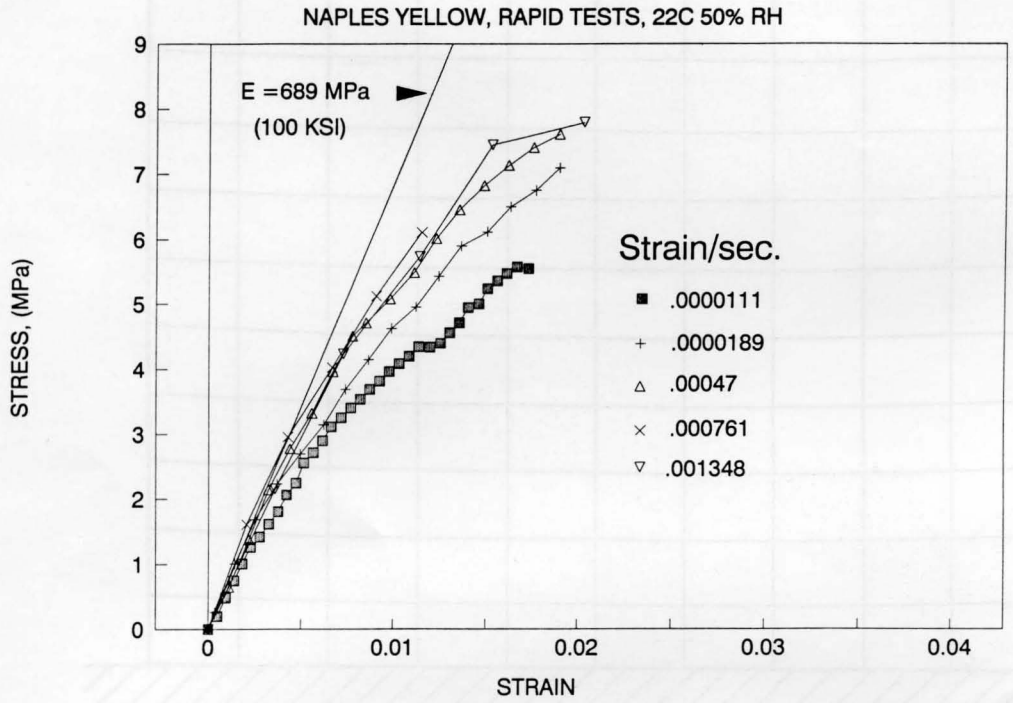

FIGURE 5
Rapid loading stress-strain results for Naples yellow paint loaded at different strain rates. There appeared to be an upper limit to the stiffness of this material since higher strain rates showed no increase in the modulus.

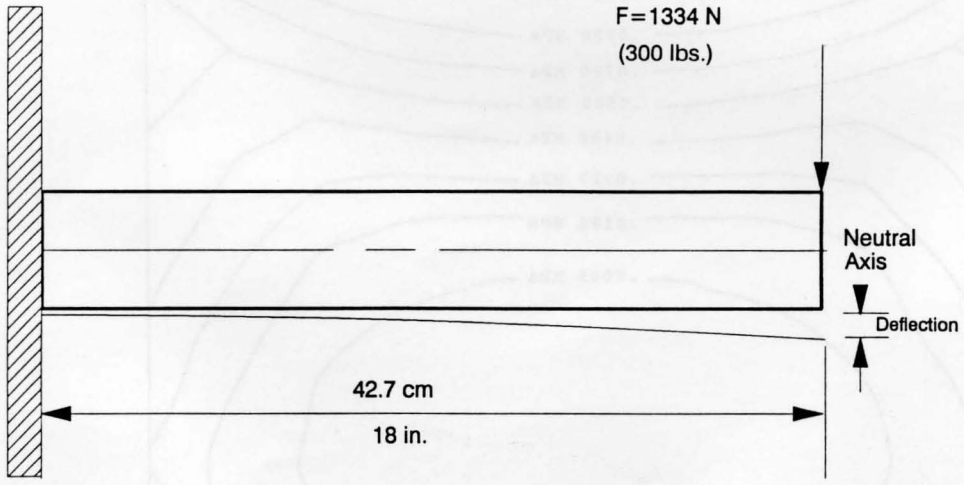

FIGURE 6
Fixed end, cantilevered beam problem run on the computer using Finite Elements. The load at the end of the beam causes a downward deflection of 1.567 cm (.617 in.) which the program computed with a difference of less than 2%.

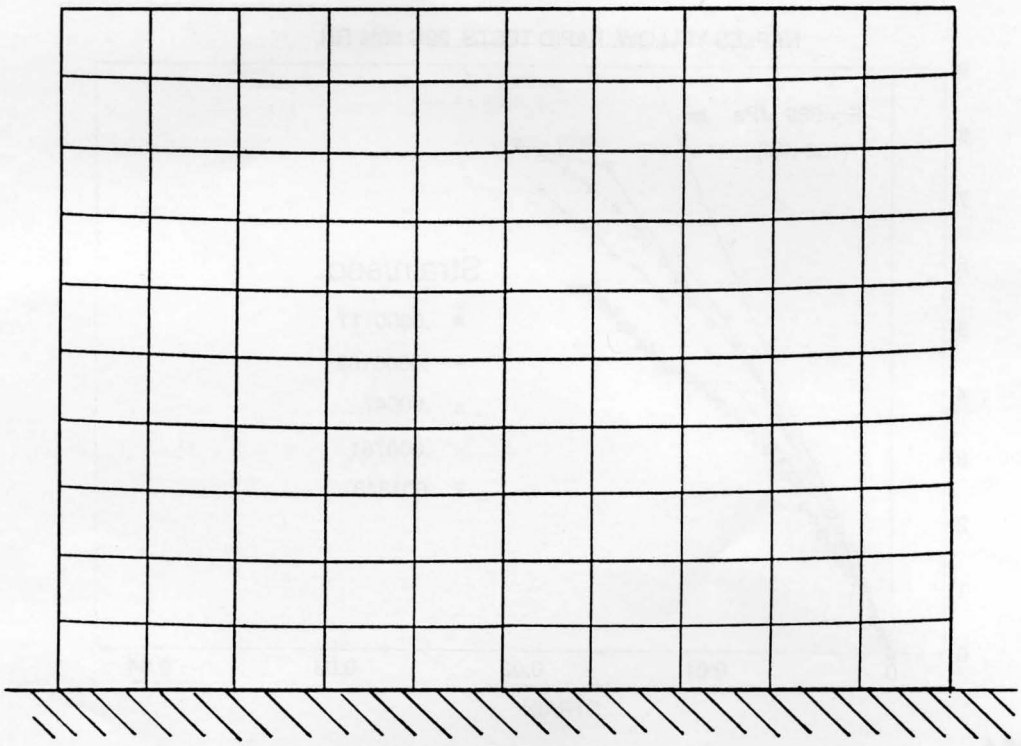

FIGURE 7
In-plane deflection of the model 76 x 102 cm painting after a 30 G impact on a flat edge. The stretcher in this model was assumed to be infinitely rigid to determine the results of the impact on the painting itself.

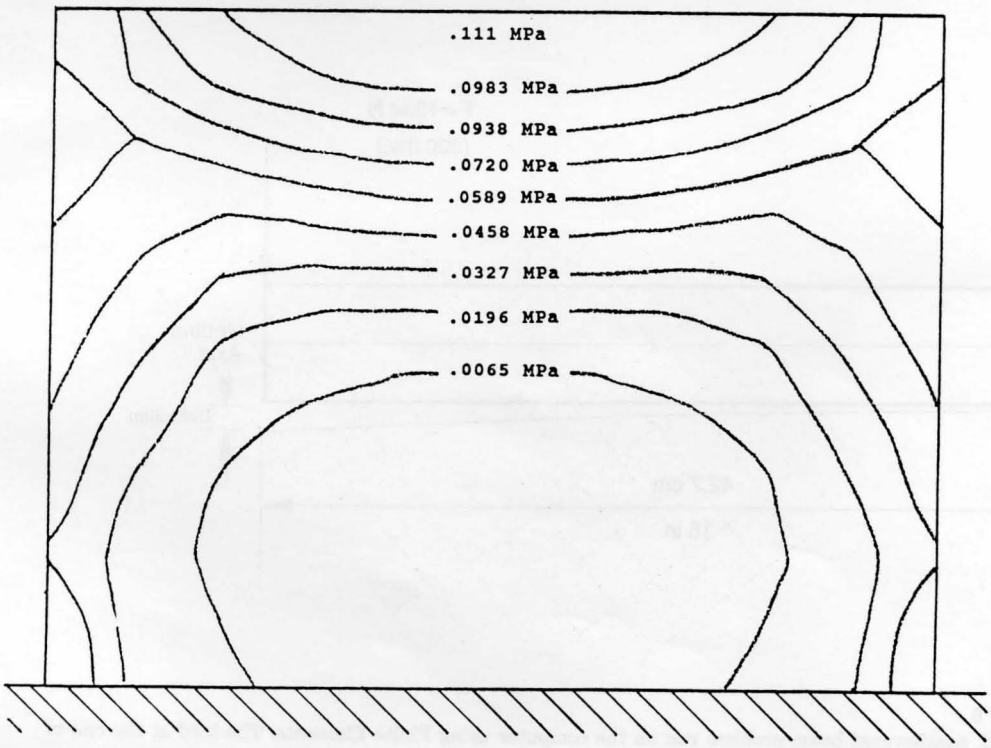

FIGURE 8
The in-plane principal stress distribution as shown on stress contours resulting from a 30 G edge impact on the 76 x 102 cm model painting. The maximum stresses are extremely low, only .11 MPa, less than 3% of the breaking strength of the white lead paint at 50% RH, 23°.

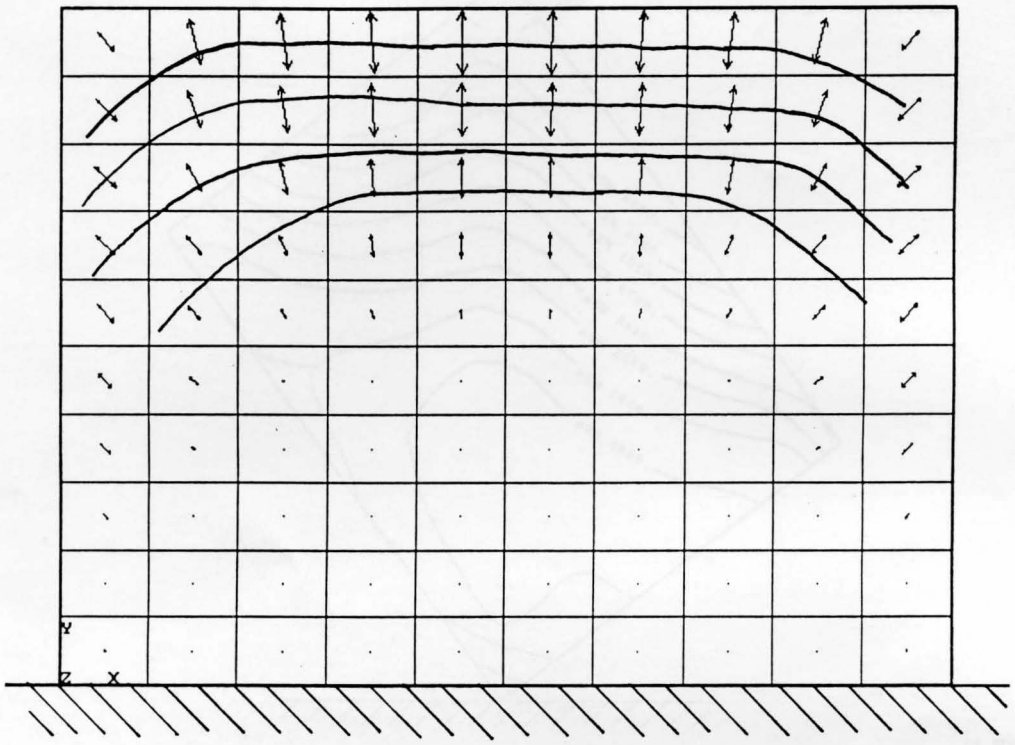

FIGURE 9
The principal stress vectors resulting from a 30 G edge impact of a 76 x 102 cm model painting. The theoretical crack pattern is superimposed over the vectors which intersect the cracks at 90 degrees.

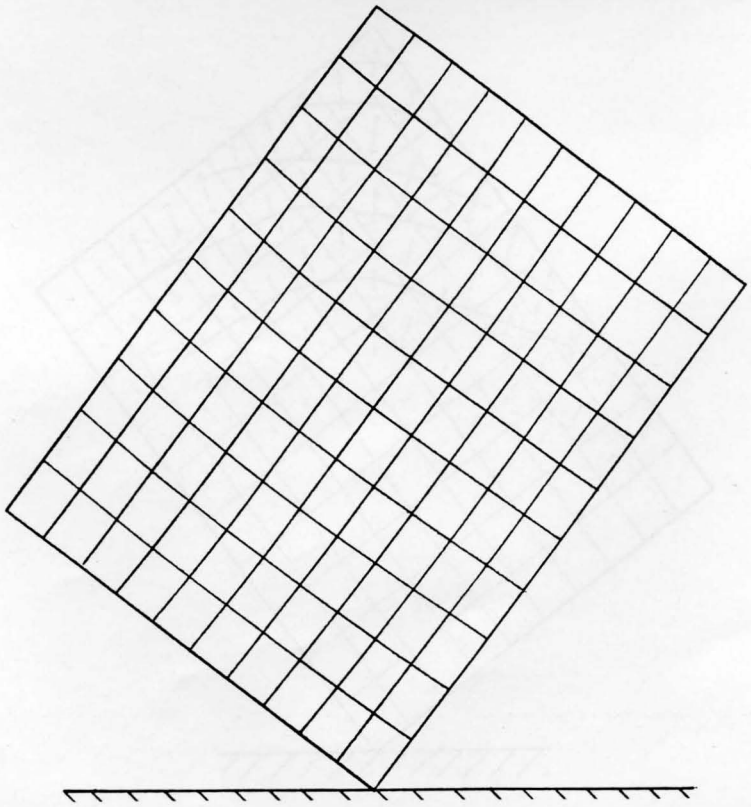

FIGURE 10
In-plane deflection of the model 76 x 102 cm painting after a 30 G impact on its corner. The stretcher in this model was assumed to be infinitely rigid to determine the results of the impact on the painting itself. The maximum deflection is quite small, only .019 cm (.0075 in.).

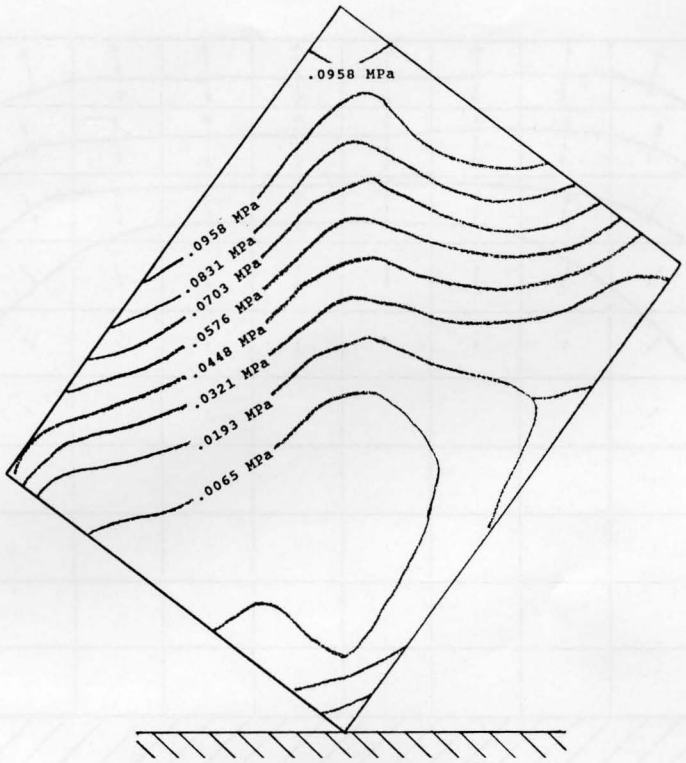

FIGURE 11
The in-plane principal stress distribution as shown on stress contours resulting from a 30 G corner impact on the 76 x 102 cm model painting. The maximum stresses are extremely low, only .11 MPa, less than 3% of the breaking strength of the white lead paint at 50% RH, 23°C.

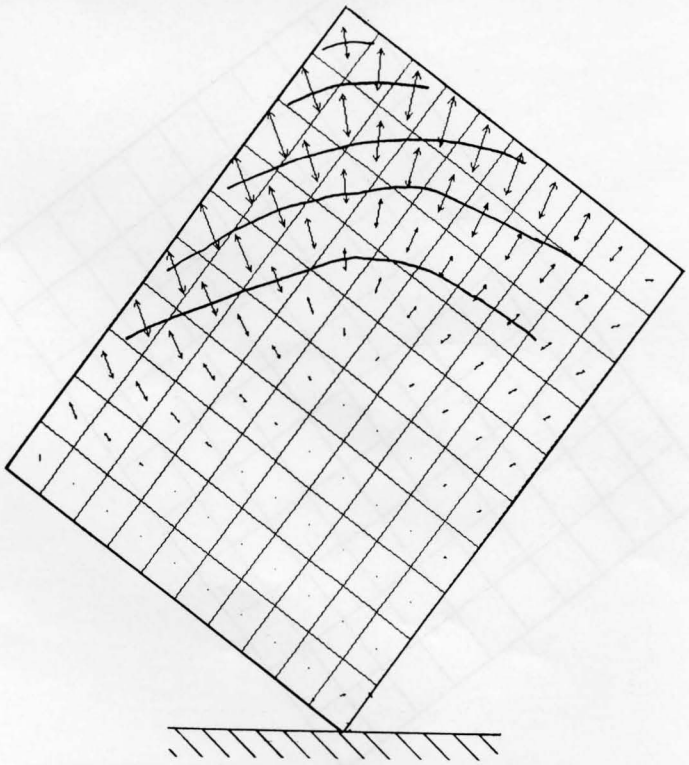

FIGURE 12
The principal stress vectors resulting from a 30 G corner impact of a 76 x 102 cm model painting. The theoretical crack pattern is superimposed over the vectors which intersect the cracks at 90 degrees.

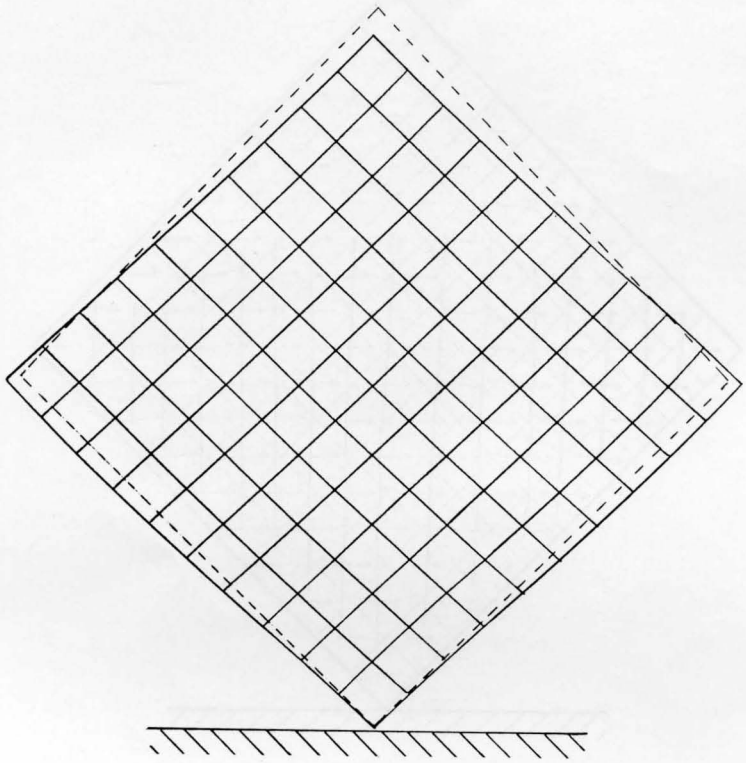

FIGURE 13
The before and after shape and displacement of a 61 x 61 cm model painting attached to a traditional wood stretcher. The corners of the stretcher were fixed. Model was subjected to a 30 G corner impact.

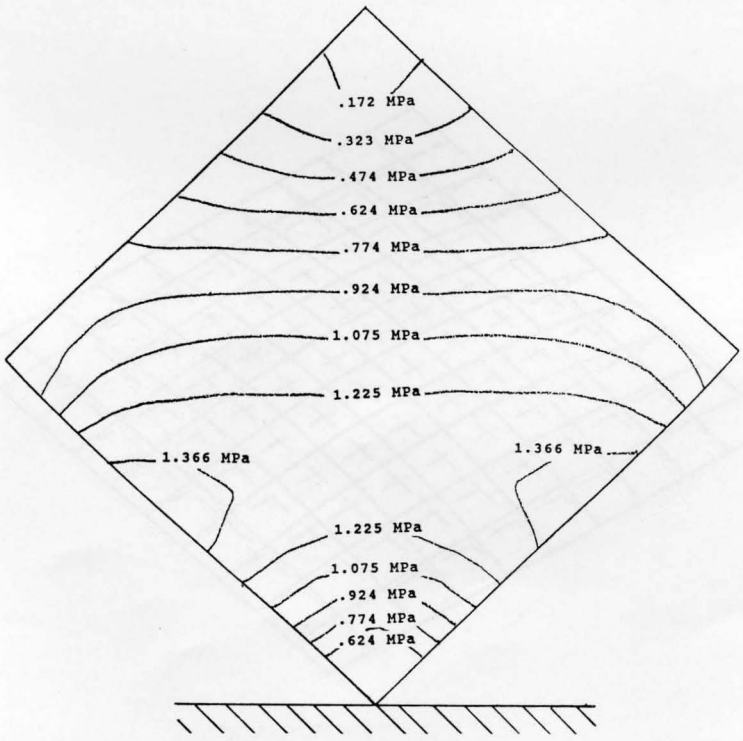

FIGURE 14
The in-plane principal stress distribution as shown on stress contours resulting from a 30 G corner impact on the 61 x 61 cm model painting. This model had a traditional wooden stretcher with fixed corners. The wood is still flexible enough to cause stresses of 1.38 MPa (.2 ksi) or 37% of the breaking strength of the white lead paint at 50% RH, 23°C.

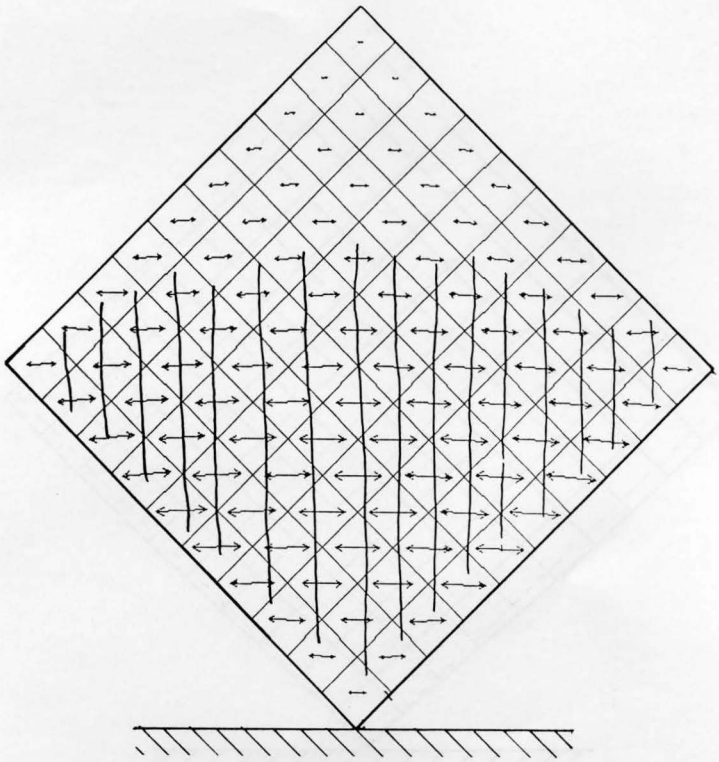

FIGURE 15
The principal stress vectors resulting from a 30 G corner impact of a 61 x 61 cm model painting with fixed corners on a wooden stretcher. The theoretical crack pattern is superimposed over the vectors which intersect the cracks at 90 degrees.

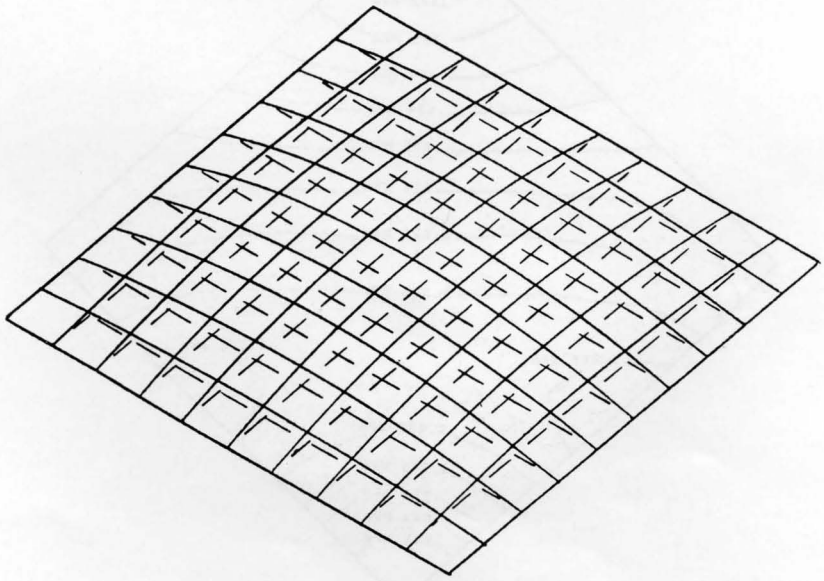

FIGURE 16
Computer generated out-of-plane displacement for a 61 x 61 cm model painting subjected to a 10 G out-of-plane acceleration.

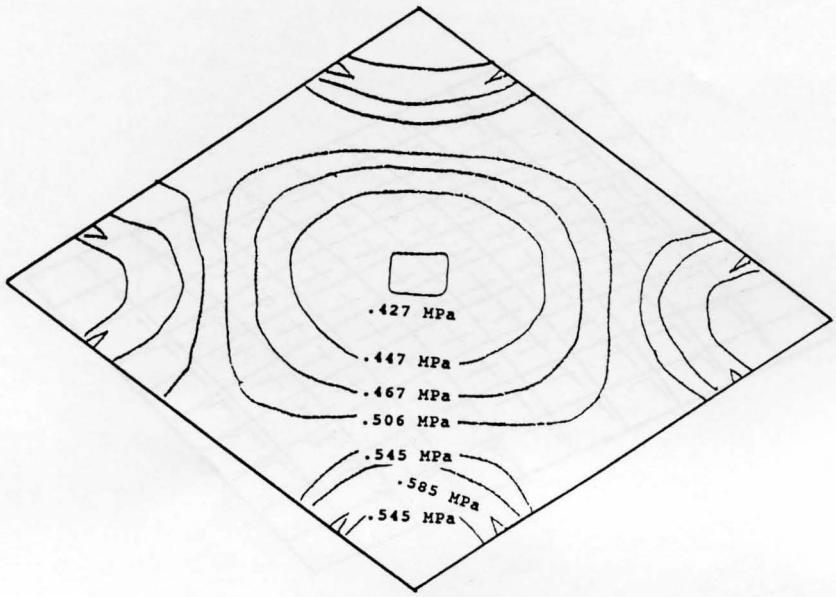

FIGURE 17
The in-plane principal stress distribution of the white lead paint layer as shown on stress contours resulting from a 10 G out-of-plane acceleration on the 61 x 61 cm model painting. The Stress is fairly uniform over the surface of the painting. The maximum stresses occur at the edges, away from the corners, and not at the center as might occur from pure bending.

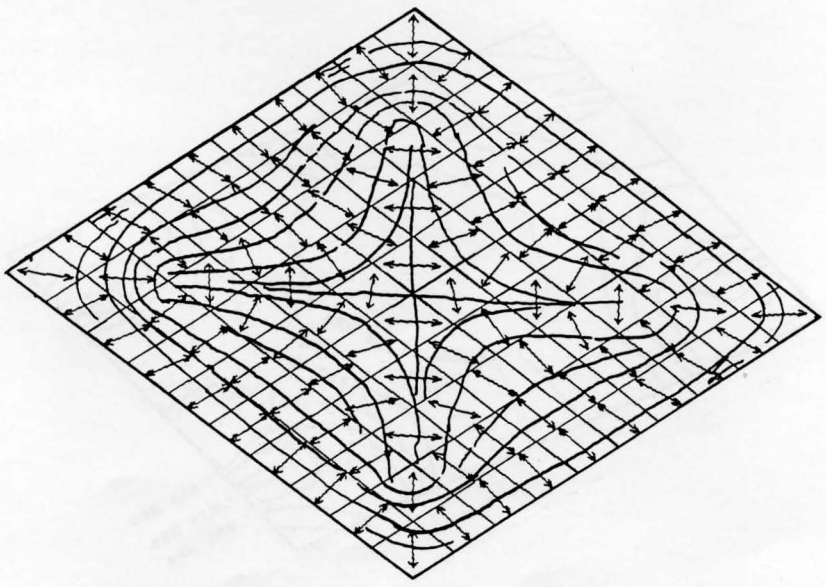

FIGURE 18
The principal stress vectors resulting from a 10 G out-of-plane acceleration of a 61 cm x 61 cm model painting. The theoretical crack pattern is superimposed over the vectors which intersect the cracks at 90 degrees.

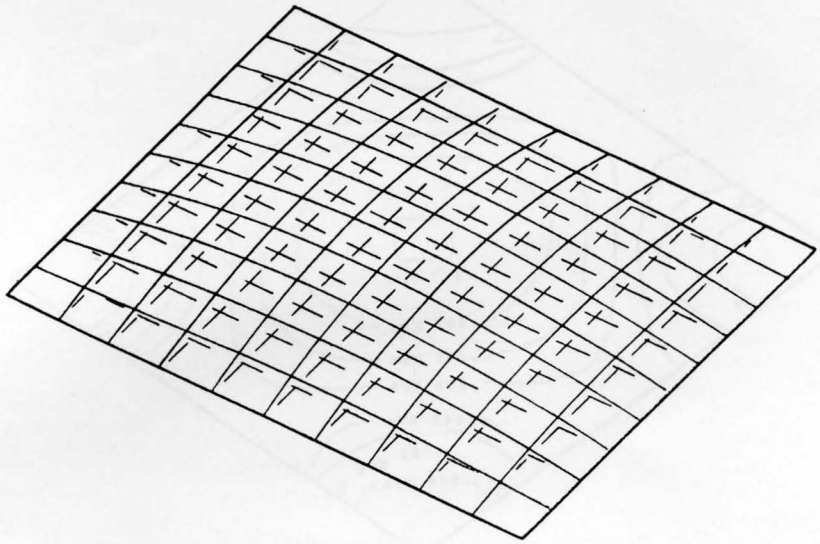

FIGURE 19
Computer generated out-of-plane displacement for a 67 x 102 cm model painting subjected to a 10 G out-of-plane acceleration.

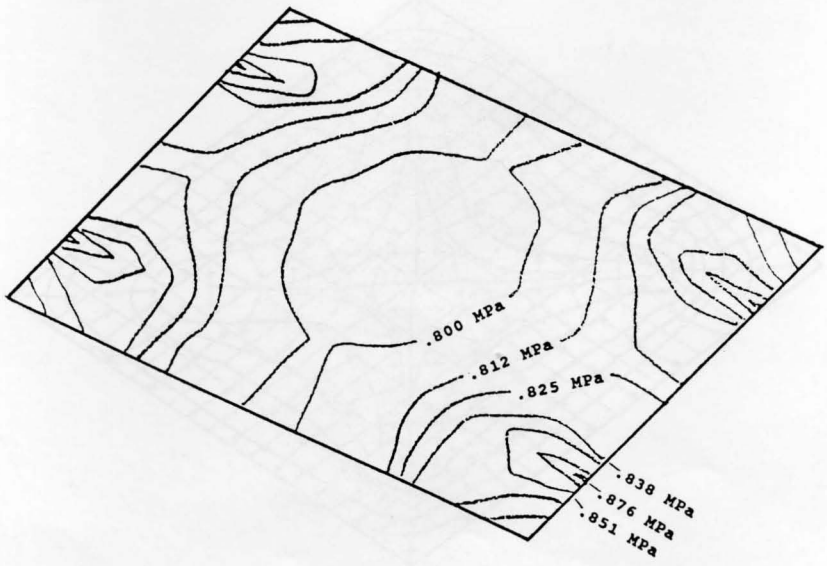

FIGURE 20
The in-plane principal stress distribution of the white lead paint layer as shown on stress contours resulting from a 10 G out-of-plane acceleration on the 67 x 102 cm model painting. The Stress is fairly uniform over the surface of the painting. The maximum stresses occur at the edges, away from the corners.

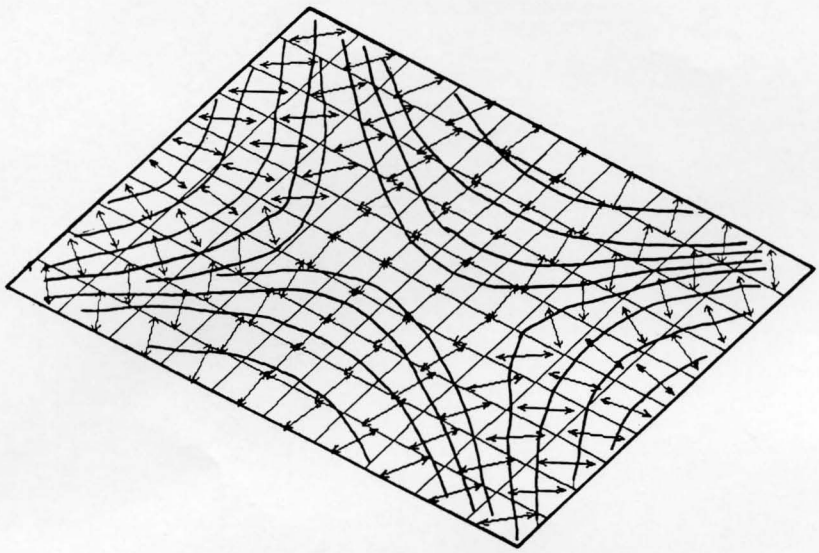

FIGURE 21
The principal stress vectors resulting from a 10 G out-of-plane acceleration of a 67 cm x 107 cm model painting. The theoretical crack pattern is superimposed over the vectors which intersect the cracks at 90 degrees. This pattern and the one in Figure 18 are not readily recognized.

APPENDIX B — TABLES

TABLE 1
Rapid test results of various 13-year-old paints at 23°C, 50% RH.

	Previously Untested			Strain Hardened	
TEST MATERIAL 23°C, 50% RH	E MPa* (KSI)**	Max σ MPa (KSI)	Max ϵ	E MPa (KSI)	Max σ MPa (KSI)
Naples Yellow Linseed Oil	689 (100)	7.58 (1.1)	.020	1172 (170)	7.58 (1.1)
Flake White Safflower Oil	689 (100)	3.72 (.54)	.0051	–	–
Vermilion Safflower Oil	737 (107)	3.86 (.56)	.0062	1241 (180)	6.06 (.88)
Burnt Sienna Linseed Oil	137.9 (20.0)	4.48 (.65)	.075	173.7 (25.2)	5.38 (.78)
Burnt Umber Linseed Oil	34.5 (5.0)	.62 (.09)	.056	–	–

* 1 KSI = 6.894 MPa ** KSI = PSI x 1000

TABLE 2
Rapid test results of various paints at 23°C.

		Previously Untested	
TEST MATERIAL 23°C, 50% RH	Age Years	RH	E MPa (KSI)
Naples Yellow Linseed Oil .043 cm thick	3.75	47	304.7 (44.2)
Naples Yellow Linseed Oil .0038 cm thick	3.75	47	327.4 (47.5)
Flake White Safflower Oil	3.75	45	413.6 (60.0)
Vermilion Safflower Oil	3.0	55	462 (67.0)
Burnt Sienna * Linseed Oil	3.75	50	0
Burnt Umber * Linseed Oil	3.75	50	0

* These paints were not dry enough to test.

TABLE 3a
The effect of RH at 23°C on the mechanical properties of 13-year-old Naples yellow.

	Previously Untested			Strain Hardened	
Naples yellow 23°C	E MPa (KSI)	Max σ MPa (KSI)	Max ϵ	E MPa (KSI)	Max σ MPa (KSI)
5% RH	1310 (190)	10.3 (1.5)	.01	1440 (209)	8.27 (1.2)
50% RH	689 (100)	7.58 (1.1)	.02	1172 (170)	7.58 (1.1)
91% RH	110 (16.0)	3.86 (.56)	.054	–	–

TABLE 3b
The effect of RH at 23°C on the mechanical properties of 13-year-old burnt sienna.

	Previously Untested			Strain Hardened	
Burnt Sienna 23°C	E MPa (KSI)	Max σ MPa (KSI)	Max ϵ	E MPa (KSI)	Max σ MPa (KSI)
5% RH	641 (93)	7.92 (1.15)	.023	561 (81.4)	6.27 (.91)
50% RH	138 (20)	4.48 (.65)	.075	174 (25.2)	5.38 (.78)
91% RH	4.48 (.65)	.31 (.045)	.064	–	–

TABLE 4a
The effect of RH at -3°C on the mechanical properties of 13-year-old Naples yellow.

Previously Untested

Naples Yellow -3° C	E MPa (KSI)	Max σ MPa (KSI)	Max ϵ
5% RH	4019 (583)	16.5 (2.4)	.0051
42% RH	2627 (381)	12.4 (1.8)	.0058
51% RH	2600 (377)	10.7 (1.55)	.0056

TABLE 4b
The effect of RH at -3°C on the mechanical proerties of 13-year-old burnt sienna.

Previously Untested

Burnt Sienna -3°C	E MPa (KSI)	Max σ MPa (KSI)	Max ϵ
5% RH	2757 (400)	16.5 (2.4)	.006
42% RH	868 (126)	11.7 (1.7)	.050
51% RH	241 (35)	5.5 (.8)	.085

TABLE 5
Rapid test of rabbit skin glue at different environments.

Rabbit Skin Glue Test Environment	E MPa (KSI)	Max σ MPa (KSI)	Max ϵ
50% RH, 23°C	4481 (650)	82.0 (11.9)	.023
5% RH, 23°C	5515 (800)	124 (18.0)	.029
5% RH, -3°C	5343 (775)	92.4 (13.4)	.019

TABLE 6
Rapid testing of gesso mixtures at 22°C and 63% RH.

Gesso to Glue Ratio by Weight	Pigment Volume Concentration	E MPa (KSI)	Max σ MPa (KSI)	Max ϵ
3.15	58.3	3200 (464)	6.51 (.945)	.0027
10.0	81.6	3757 (545)	5.75 (.835)	.0021
13.3	85.5	4136 (600)	4.66 (.676)	.0012
15.0	86.9	4101 (595)	4.66 (.677)	.0013
20.0	89.9	2088 (303)	2.54 (.368)	.0012
30.0	93.0	1709 (248)	1.17 (.170)	.00061

TABLE 7
Measured average fiber cross sections per yarn for the test linens.

	Warp	Weft		Warp	Weft
Fabric	Area of Yarns cm^2 $in.^2$	Area of Yarns cm^2 $in.^2$	Fabric Weight N/cm^2 $oz./in.^2$	Yarn Count no./cm no./in.	Yarn Count no./cm no./in.
#248	.00057 .000088	.00048 .000074	.000398 .00924	24.6 62.5	20.2 51.5
#444	.00052 .000080	.00043 .000066	.000347 .00897	24.4 62.0	19.3 49.0
#8800	.00050 .000078	.00052 .000080	.000268 .00622	16.7 42.5	15.4 39.1

TABLE 8
Mean fiber modulus versus relative humidity for a typical linen textile.

Relative Humidity %	Warp Direction, E MPa (KSI)	Weft Direction, E MPa (KSI)
18	24.1 (3.5)	289 (42)
40	-	675 (98)
48	24.1 (3.5)	-
59	-	758 (110)
70	68.9 (10)	-
75	-	2275 (330)
91	213 (30.9)	-
93	-	1585 (230)
95	606 (88)	-
Saturated	510 (74)	-

TABLE 9a
Comparison of the FEA analysis results wity the theoretical free-end deflection for the cantilevered beam problem.

Number of Elements	Theoretical Solution/cm	Finite Element Solution/cm	% Difference
1	1.567	.104	93
4	1.567	.348	77
72	1.567	1.33	15
180	1.567	1.45	4
360	1.567	1.557	1.2

TABLE 9b
Comparison of the FEA analysis results with the theoretical stresses when 360 elements were used.

Maximum Stresses	Theoretical MPa (KSI)	FEA Results MPa (KSI)	% Difference
Bending	26.1 (3.79)	26.8 (3.89)	-2.6
Shear	1.09 (.158)	1.07 (.155)	1.9

TABLE 10
Nominal weight densities for typical artists' materials.

Material	Nominal Density N/cm^3	Nominal Density $Lbs./in.^3$
White Lead Paint	.0279	.1029
Naples Yellow Paint	.0254	.0936
Burnt Sienna Paint	.0206	.0757
Rabbit Skin Glue	.01	.0368
Gesso, PVC = 58.3	.0128	.0473
Gesso, PVC = 89.9	.0101	.0374
Linen #248	.00628	.0231
Linen #444	.00546	.0201
Linen #8800	.00555	.0201
Oak, average	.00979	.03605

TABLE 11
Maximum stresses from a 10 G acceleration at different initial tensions for the 61 x 61 cm painting.

Initial Fabric Stress MPa (KSI)	Initial Glue Stress MPa (KSI)	Initial Paint Stress MPa (KSI)	10G Fabric Stress MPa (KSI)	10G Glue Stress MPa (KSI)	10G Paint Stress MPa (KSI)	10G Max. Def. cm (in.)
.316 (.458)	2.05 (.298)	.317 (.046)	.593 (.086)	3.81 (.552)	.586 (.085)	.703 (.277)
.345 (.050)	2.24 (.325)	.345 (.050)	.634 (.092)	4.10 (.595)	.627 (.091)	.592 (.233)
.434 (.063)	2.80 (.406)	.434 (.063)	.730 (.106)	4.71 (.683)	.724 (.105)	.475 (.187)
.572 (.083)	3.73 (.541)	.572 (.083)	.916 (.133)	5.92 (.859)	.910 (.132)	.358 (.141)

TABLE 12
The effects of increasing out-of-plane acceleration on the 67 x 102 cm painting at a fixed initial tension.

Acceleration	Fabric Stress MPa (KSI)	Glue Stress MPa (KSI)	Paint Stress MPa (KSI)	Deflection cm (in.)
1G	.799 (.116)	5.14 (.745)	.79 (.115)	.066 (.026)
5G	.813 (.118)	5.26 (.763)	.813 (.118)	.39 (.156)
10G	.89 (.129)	5.73 (.831)	.88 (.128)	.81 (.317)

TABLE 13
The effects of desiccation and chilling while applyhing a 10 G acceleration to the 67 (30) x 102 cm (40 in.) painting.

Initial Stresses			Total Stresses @ 10 G			
Fabric Stress MPa (ksi)	Glue Stress MPa (KSI)	Paint Stress MPa (KSI)	Fabric Stress MPa (ksi)	Glue Stress MPa (KSI)	Paint Stress MPa (KSI)	Def. cm in.
.648 (.094)	4.13 (.600)	2.98 (.432)	1.03 (.149)	6.55 (.95)	4.76 (.690)	.424 (.167)

TABLE 14
Maximum computed stresses for a painting with gesso replacing the white lead paint at a 10 G acceleration.

Initial Stresses			Total Stresses @ 10 G			
Fabric Stress MPa (ksi)	Glue Stress MPa (KSI)	Gesso Stress MPa (KSI)	Fabric Stress MPa (ksi)	Glue Stress MPa (KSI)	Gesso Stress MPa (KSI)	Def. cm (in.)
.276 (.040)	1.79 (.260)	.684 (.099)	.593 (.086)	3.82 (.554)	1.45 (.211)	.973 (.383)

ACKNOWLEDGMENTS

We wish to thank the Scholarly Studies Program of the Smithsonian Institution for its generous support of this research project.

NOTES

1. A. Elm, "Some Mechanical Properties of Paint Films," *Official Digest*, 25 (1953), 750-774; A. C. Elm, "The Stress-Strain Properties of Clear and Pigmented Films of Pure Drying Oil Compounds," *Official Digest*, (1951), 701-723; M. G. Shiker, "Deformation Properties of Linseed Oil Films," *Journal of Applied Chemistry*, (USSR), 12 (1932), 1884-1891; A. V. Damfilov and Ye. G. Ivancheva, "Mechanical Properties of Pigmented Oil Films," *Journal of Applied Chemistry* (USSR) 20 (1947), 676-683; A. Toussaint and L. D'Hont, "Ultimate Strength of Paint Films," *J. Oil Col. Chem. Assoc.* 64 (1981), 302-307; A. Zosel, "Mechanical Behavior of Coating Films," *Progress in Organic Coatings* 8 (1980), 47-79; Kozo Sato, "The Mechanical Properties of Filled Polymers," *Progress in Organic Coatings* 4 (1976), 271-302; M. F. Mecklenburg, "Some Aspects of the Mechanical Behavior of Fabric Supported Paintings," Report to the Smithsonian Institution (1982), 7-12; G. Hedley, M. Odlyha, A. Burnstock, J. Tillinghast, and C. Husband, "A Study of the Mechanical and Surface Properties of Oil Paint Films Treated with Organic Solvents and Water," *IIC Preprints* of the contributions to the Brussels Congress (1990), 98-105.

2. J. M. Ward, *Mechanical Properties of Solid Polymers* (1983); P. Mears, Polymers, *Structure and Bulk Properties* (1967); M. F. Mecklenburg, Ph.D. Dissertation, University of Maryland (1984), 15-20.

3. H. D. Ferry, *Viscoelastic Properties of Polymers* (1961).

4. *Wood Handbook, Wood as an Engineering Material,* USDA Agricultural Handbook No. 72 (1974); R. B. Hoadley, *Understanding Wood, A Craftsman's Guide to Wood Technology* (1981); P. Koch, *Utilization of Southern Pine, Volumes I and II,* USDA Agricultural Handbook No. 420 (1977), F.F.P. Kollmann and W. A. Côte, Jr., *Principles of Wood Science and Technology, Volume I, Solid Wood* (1986), 321-405.

5. Mecklenburg 1984, 10.

6. M. F. Mecklenburg and C. S. Tumosa, "Mechanical Properties of Paintings Subjected to Changes in Temperature and Relative Humidity," elsewhere in this publication; M. F. Mecklenburg, "The Effects of Atmospheric Moisture on the Mechanical Properties of Collagen Under Equilibrium Conditions," *AIC Preprints of Papers Presented at the 16th Annual Meeting* (1988), 231-244.

7. Analysis of this paint was conducted at CAL by W. D. Erhardt and W. Hopwood, unpublished research, (1990).

8. H. Lee and K. Neville, *Handbook of Epoxy Resins* (1967); Mecklenburg 1984, 15-20.

9. K. Wehlte, *The Materials and Techniques of Painting with a Supplement on Color Theory* (1975), 348-354; R. Mayer, *The Artist's Handbook of Materials and Techniques* (1980), 256; A. P. Laurie, *The Painter's Methods and Materials* (1967), 66.

10. See note 4.

11. Wehlte 1975, 326-331.

12. A. J. Panshin and C. de Zeeuw, *Textbook of Wood Technology* (1980), 223-225.

13. R. D. Cook, *Concepts and Applications of Finite Element Analysis* (1974), 173-188; J. S. Przemieniecki, *Theory of Matrix Structural Analysis* (1968), 102-122.

14. S. P. Timoshenko and J. N. Goodier, *Theory of Elasticity* (1970) 361-366; E. J. Hearn, *Mechanics of Materials* (1977), 57-72.

15. P. J. Marcon, "Shock, Vibration and Protective Package Design," elsewhere in this publication (1991).

16. P. J. Marcon, "Shock, Vibration and the Shipping Environment," elsewhere in this publication (1991).

17. P. J. Marcon, Canadian Conservation Institute, private communication; C. M. Harris, *Shock & Vibration Handbook* (1988); F. E. Ostrem and B. Liboviez, "A Survey of Environmental Conditions Incident to the Transportation of Materials," Final Report, PB 204 442, prepared for USDOT (1971); "An Assessment of the Common Carrier Shipping Environment," General Technical Report FPL 22, USDA Forest Products Laboratory (1979).

18. Hedley 1990.